Automatica 127 (2021) 109501

Contents lists available at ScienceDirect

Automatica

journal homepage: www.elsevier.com/locate/automatica

Connectivity-maintaining and collision-avoiding performance function approach for robust leader–follower formation control of multiple uncertain underactuated surface vessels☆

Bong Seok Park [a], Sung Jin Yoo [b,*]

[a] Department of Future Convergence Engineering, Kongju National University, Cheonan 31080, South Korea
[b] School of Electrical and Electronics Engineering, Chung-Ang University, 84 Heukseok-Ro, Dongjak-Gu, Seoul 156-756, South Korea

ARTICLE INFO

Article history:
Received 19 August 2019
Received in revised form 27 August 2020
Accepted 22 December 2020
Available online 8 February 2021

Keywords:
Leader–follower formation control
Connectivity maintenance
Collision and obstacle avoidances
Underactuated surface vessels (USVs)
Unknown nonlinearities

ABSTRACT

A robust leader–follower formation tracking design using connectivity-maintaining and collision-avoiding performance functions is developed for multiple uncertain underactuated surface vessels (USVs). It is assumed that the USVs communicate within limited ranges and all nonlinearities of the USV dynamics are completely unknown. Compared with the related literature, two primary contributions of this paper are to derive connectivity-maintaining and collision-avoiding performance functions for designing a robust formation tracking scheme using only relative state information and to establish an obstacle avoidance strategy guaranteeing the connectivity between the leader and the followers while avoiding an obstacle. Based on the Lyapunov stability theorem, the predesignated formation tracking performance and stability of the proposed control system have been analyzed without using potential-like functions and function approximation techniques. Simulation results are provided to show the effectiveness of the proposed theoretical result.

1. Introduction

The control problem of unmanned surface vessels has been getting a lot of attention due to the advantage of being able to perform tasks such as transportation, exploration, and reconnaissance without human involvement. In particular, since these unmanned surface vessels are underactuated systems that have actuators only for surge and yaw and no actuator that can move sideways (sway) (Moe & Pettersen, 2016), it is difficult to design control systems. As a result, many researchers have proposed several control approaches (see Chen et al., 2019; Dai et al., 2019; Park et al., 2017; Qin et al., 2019; Sun, Zhang, Yang et al., 2018; Xie et al., 2018 and the references therein). In addition, in order to perform various unmanned missions, it is more efficient to operate multiple underactuated surface vessels (USVs) than a single USV. Therefore, several studies for operating multiple USVs have appeared in Do (2011), Huang et al. (2019), Xie and Ma (2018) and Yoo and Park (2017). Especially, the leader–follower formation approaches for multiple USVs have actively been presented in Cui et al. (2010), Park (2015), Shojaei (2015) and Sun, Zhang, Lu et al. (2018). Although the existing leader–follower formation results (Cui et al., 2010; Park, 2015; Shojaei, 2015; Sun, Zhang, Lu et al., 2018) can successfully operate multiple USVs, there are two more essential elements for practical operation of multiple USVs in the leader–follower formation approach. One is connectivity maintenance due to the physical limitations of communications and sensors, and the other is collision avoidance for successful mission performance (Sakai et al., 2018).

To address connectivity maintenance issues under limited communication and sensing ranges, Fiedler value (Fiedler, 1973) based methods were proposed in Gennaro and Jadbabaie (2016) and Sabattini et al. (2013). Zavlanos et al. (2009) presented a flocking algorithm to achieve speed matching of networked agents. In Ajorlou et al. (2010) and Su et al. (2010), the potential functions were used to obtain a bounded consensus control and to solve the consensus problem preserving connectivity, respectively. In order to maintain the connectivity of multiple robots, rendezvous algorithms were proposed in Cortés et al. (2006) and Dong (2016) and a bounded control strategy was presented in Ajorlou and Aghdam (2013). However, the studies mentioned above do not deal with the collision avoidance problem. If the agents do a maneuver to avoid collisions, the distance between

☆ This work was supported by the National Research Foundation of Korea (NRF) grant funded by the Korean government Grant NRF-2019R1A2C1087552 and Grant NRF-2019R1A2C1004898. The material in this paper was not presented at any conference. This paper was recommended for publication in revised form by Associate Editor Michael M. Zavlanos under the direction of Editor Christos G. Cassandras.

* Corresponding author.
E-mail addresses: bspark@kongju.ac.kr (B.S. Park), sjyoo@cau.ac.kr (S.J. Yoo).

https://doi.org/10.1016/j.automatica.2021.109501
0005-1098/

the agents can be farther away and thus can get out of limited communication and sensing ranges. Therefore, the collision avoidance problem must be addressed along with connectivity preservation issues. As some remedies on this problem, connectivity preservation issues in an obstacle environment were addressed in Ganguli et al. (2009) and Li et al. (2013), and Sakai et al. (2018) proposed an algorithm that considers both collision avoidance of internal robots and obstacle avoidance of robots. Despite these efforts, some limited research results have been reported for the formation control problem related to the collision avoidance and connectivity preservation of multiple USVs. In Ghommam and Saad (2018), an adaptive leader–follower formation control using barrier Lyapunov functions was presented for a group of USVs with range and bearing constraints. Recently, a unified error transformation method without using the potential function was proposed for the connectivity-preserving and collision-avoiding formation control of USVs (Park & Yoo, 2019). However, the previous formation results (Ghommam & Saad, 2018; Park & Yoo, 2019) for multiple uncertain USVs have the following issues for more improvement.

(I-1) The collision avoidance problem between USVs and the obstacle was not considered in Ghommam and Saad (2018) and Park and Yoo (2019). The followers with limited communication ranges should avoid an obstacle while preserving the connectivity to the leader. To the best of our knowledge, this issue is still open in the formation control field of USVs.

(I-2) The compensation of model uncertainties reported in Ghommam and Saad (2018) and Park and Yoo (2019) was based on adaptive and function approximation techniques that lead to the complexity of the formation control system owing to the online implementation of differential equations (i.e., adaptive laws).

These two issues motivate us to resolve the problem of connectivity maintenance and collision and obstacle avoidances for multiple uncertain USVs within the framework of the leader–follower formation approach.

The aim of this paper is to develop a leader–follower-approach-based robust formation control design with low complexity of multiple uncertain USVs while preserving connectivity and avoiding collisions with the USVs and the obstacle. This development has been done by designing a novel formation error using connectivity-maintaining and collision-avoiding performance functions, different from existing performance functions reported in Bechlioulis and Rovithakis (2014) for setting the bounds of only prescribed tracking performance. The recursive design strategy based on the proposed formation error is established to design robust underactuated control laws (i.e., surge force and yaw moment laws) using only relative state information for each USV with uncertain nonlinear dynamics. We also propose a strategy to avoid collision with the obstacle while maintaining the distance from the leader robot to preserve connectivity. All of these features are accomplished through a single controller for each USV that need not use additional techniques such as switching control. Based on the Lyapunov stability theorem, the predesignated formation tracking performance and stability of the proposed control system have been analyzed without using potential-like functions and function approximation techniques.

The contributions of this paper are summarized as follows.

(C-1) In contrast to Ghommam and Saad (2018) and Park and Yoo (2019), both collisions between the USVs and collisions with the obstacle can be avoided by implementing a single controller for each USV follower and designing a new formation error function for avoiding collisions and maintaining connectivity between the leader and the followers.

(C-2) Compared with Ghommam and Saad (2018) and Park and Yoo (2019), the structure of the leader–follower formation controller can be simplified because it does not include any adaptive parameters and function approximators although the nonlinearities in the dynamics of USV are completely unknown. Also, the bounds of the formation tracking performance can be predesignated by adjusting preselected design parameters.

(C-3) Compared with the existing prescribed-performance-based low-complexity control design (Bechlioulis & Rovithakis, 2014), this paper presents a new formation error using connectivity-maintaining and collision-avoiding performance functions. The recursive leader–follower formation design and its stability analysis strategy for multiple uncertain USVs are established via the proposed formation error.

Advantages and motivations: Compared with the previous works (Atinç et al., 2013; Giordano et al., 2013; Jin et al., 2015; Karkoub et al., 2019; Poonawala et al., 2015), the main advantages and motivations of our paper are as follows:

(i) The four problems (i.e, the connectivity preservation among agents, the collision avoidance among agents, the obstacle avoidance while preserving the connectivity among agents, distributed formation tracking) considered in our paper cannot simultaneously be handled in Atinç et al. (2013), Giordano et al. (2013), Jin et al. (2015), Karkoub et al. (2019), and Poonawala et al. (2015) where the connectivity preservation problem among mobile robots was not considered in Jin et al. (2015), the collision avoidance problem was not considered in Giordano et al. (2013), and the obstacle avoidance problem was not considered in Atinç et al. (2013), Karkoub et al. (2019), and Poonawala et al. (2015).

(ii) The potential functions used in Atinç et al. (2013), Giordano et al. (2013), Karkoub et al. (2019), and Poonawala et al. (2015) should be individually and differently designed according to the connectivity preservation and collision avoidance objectives in the robot formation problem. The desired velocities for the control purposes are derived from the derivatives of the potential functions. The total control input is combined with a control input for each purpose (please see (16) in Poonawala et al. (2015)). Thus, it can cause the local minimum problem due to the derivatives of different potential functions. However, our formation control approach is independent of potential functions.

(iii) In Jin et al. (2015), the unified velocity method that switches the desired velocity between the attractive and avoidance modes was presented to ensure the collision avoidance. This method can solve the local minimum problem, but it can lose the connectivity of the robots due to collision avoidance maneuvers. To solve this problem, we propose a new approach that can ensure the connectivity preservation and collision avoidance of USVs without using the potential functions. The key idea is to design the new unified error signal using the performance functions. In addition, different from the existing works (Atinç et al., 2013; Giordano et al., 2013; Jin et al., 2015; Karkoub et al., 2019; Poonawala et al., 2015), the exponentially decaying performance functions can also guarantee the predesignated formation tracking performance of USVs and the obstacle avoidance strategy maintains the connectivity among USVs while avoiding the obstacle.

(iv) In Atinç et al. (2013), Jin et al. (2015), Karkoub et al. (2019), and Poonawala et al. (2015), the kinematic model of nonholonomic mobile robots was only considered to design collision-free and connectivity preserving formation control systems, without considering the nonlinear dynamics

of robots. Furthermore, the kinematic and the dynamic property of the USVs are different from those of nonholonomic mobile robots. In addition, floating masses storing kinetic energy was only considered in Giordano et al. (2013). However, the system considered in Giordano et al. (2013) does not have the underactuated property. Thus, these previous formation control designs cannot be applied to our problem, even in the concerned model respects.

2. Problem formulation

Consider USVs with limited communication and sensing ranges. Throughout the paper, the leader is denoted with a subscript "j" and the follower is denoted by the subscript "i". The model of the USV follower i is described by (Do & Pan, 2005)

$$\dot{q}_i = \begin{bmatrix} \cos\psi_i & -\sin\psi_i & 0 \\ \sin\psi_i & \cos\psi_i & 0 \\ 0 & 0 & 1 \end{bmatrix} \varpi_i, \tag{1}$$

$$\dot{\varpi}_i = h_i(u_i, v_i, r_i) + d_i + \begin{bmatrix} \tau_{i,u}/m_{i,11} \\ -m_{i,23}\tau_{i,r}/\Delta_i \\ m_{i,22}\tau_{i,r}/\Delta_i \end{bmatrix}, \tag{2}$$

where $q_i = [x_i, y_i, \psi_i]^\top$; x_i, y_i, and ψ_i denote the positions and orientation in the Earth-fixed frame, $\varpi_i = [u_i, v_i, r_i]^\top$; u_i, v_i, and r_i denote the surge, sway and yaw velocities of the USV in the body-fixed frame, $d_i = [d_{i,1}, d_{i,2}, d_{i,3}]^\top$; $d_{i,1}$, $d_{i,2}$, and $d_{i,3}$ are external disturbances, $\tau_{i,u}$ and $\tau_{i,r}$ are control inputs denoting the surge force and yaw moment, respectively, and $h_i = [h_{i,1}, h_{i,2}, h_{i,3}]^\top$; $h_{i,1}$, $h_{i,2}$, and $h_{i,3}$ are *completely unknown* nonlinear functions including the hyrodynamic coefficients defined by

$$\begin{aligned}
h_{i,1} &= \frac{1}{m_{i,11}}\{m_{i,22}v_i r_i + m_{i,t} r_i^2 - \kappa_{i,11}u_i\}, \\
h_{i,2} &= \frac{1}{\Delta_i}[\{m_{i,22}m_{i,23} - m_{i,11}m_{i,23}\}u_i v_i \\
&\quad + \{m_{i,23}m_{i,t} - m_{i,11}m_{i,33}\}u_i r_i \\
&\quad + \{\kappa_{i,33}r_i + \kappa_{i,32}v_i\}m_{i,23} \\
&\quad - \{\kappa_{i,23}r_i + \kappa_{i,22}v_i\}m_{i,33}], \\
h_{i,3} &= \frac{1}{\Delta_i}[\{m_{i,11}m_{i,22} - m_{i,22}^2\}u_i v_i \\
&\quad + \{m_{i,11}m_{i,32} - m_{i,t}m_{i,22}\}u_i r_i \\
&\quad - \{\kappa_{i,33}r_i + \kappa_{i,32}v_i\}m_{i,22} \\
&\quad + \{\kappa_{i,23}r_i + \kappa_{i,22}v_i\}m_{i,32}],
\end{aligned}$$

with $\Delta_i = m_{i,22}m_{i,33} - m_{i,23}m_{i,32}$, $m_{i,11} = m_i - P_{i,\dot{u}_i}$, $m_{i,22} = m_i - Q_{i,\dot{v}_i}$, $m_{i,23} = m_i x_{i,g} - Q_{i,\dot{r}_i}$, $m_{i,32} = m_i x_{i,g} - N_{i,\dot{v}_i}$, $m_{i,33} = I_{i,z} - N_{i,\dot{r}_i}$, $m_{i,t} = (m_{i,23} + m_{i,32})/2$, $\kappa_{i,11} = -(P_{i,u} + P_{i,u|u|}|u_i|)$, $\kappa_{i,22} = -(Q_{i,v} + Q_{i,|v|v}|v_i| + Q_{i,|r|v}|r_i|)$, $\kappa_{i,23} = -(Q_{i,r} + Q_{i,|v|r}|v_i| + Q_{i,|r|r}|r_i|)$, $\kappa_{i,32} = -(N_{i,v} + N_{i,|v|v}|v_i| + N_{i,|r|v}|r_i|)$, and $\kappa_{i,33} = -(N_{i,r} + N_{i,|v|r}|v_i| + N_{i,|r|r}|r_i|)$.

Here, m_i is the mass of the USV follower i, $P_{i,\dot{u}}$, $Q_{i,\dot{v}}$, $Q_{i,\dot{r}}$, $N_{i,\dot{v}}$ and $N_{i,\dot{r}}$ are added masses of the USV follower i, $P_{i,u}$, $P_{i,u|u|}$, $Q_{i,v}$, $Q_{i,|v|v}$, $Q_{i,|r|v}$, $Q_{i,r}$, $Q_{i,|v|r}$, $Q_{i,|r|r}$, $N_{i,v}$, $N_{i,|v|v}$, $N_{i,|r|v}$, $N_{i,r}$, $N_{i,|v|r}$, and $N_{i,|r|r}$ denote linear and quadratic drag coefficients, $I_{i,z}$ is the inertia with respect to the vertical axis, and $x_{i,g}$ is the center of gravity of the USV follower i in the body-fixed frame.

For the leader–follower formation control, it is generally assumed that one of USVs is the global leader that tracks a given path, each USV regards one of USVs, that is included within its limited communication and sensing ranges, as its leader, the USV followers can receive the information of the leader within only their limited communication and sensing ranges, and the graph connectivity of the total USVs has a directed spanning tree with the root node being the global leader.

As shown in (2), the yaw moment $\tau_{i,r}$ appears in both the sway and yaw dynamics. This property makes the controller design difficult. To address this problem, the following state transformations are employed (Do & Pan, 2005): $\bar{x}_i = x_i + \zeta_i \cos\psi_i$, $\bar{y}_i = y_i + \zeta_i \sin\psi_i$, and $\bar{v}_i = v_i + \zeta_i r_i$ where $\zeta_i = m_{i,23}/m_{i,22}$, $i = 1, \ldots, N$. Then, (1) and (2) are transformed by

$$\begin{aligned}
\dot{\bar{x}}_i &= u_i \cos\psi_i - \bar{v}_i \sin\psi_i, \\
\dot{\bar{y}}_i &= u_i \sin\psi_i + \bar{v}_i \cos\psi_i, \\
\dot{\psi}_i &= r_i, \\
\dot{u}_i &= h_{i,1}(u_i, \bar{v}_i, r_i) + d_{i,1} + \tau_{i,u}/m_{i,11}, \\
\dot{\bar{v}}_i &= \bar{h}_{i,2}(u_i, \bar{v}_i, r_i) + \bar{d}_{i,2}, \\
\dot{r}_i &= h_{i,3}(u_i, \bar{v}_i, r_i) + d_{i,3} + m_{i,22}\tau_{i,r}/\Delta_i,
\end{aligned} \tag{3}$$

where $\bar{h}_{i,2} = h_{i,2} + \zeta_i h_{i,3}$ and $\bar{d}_{i,2} = d_{i,2} + \zeta_i d_{i,3}$. As stated in Skjetne et al. (2005), it is difficult to find $\kappa_{i,11}$, $\kappa_{i,22}$, $\kappa_{i,23}$, $\kappa_{i,32}$, and $\kappa_{i,33}$ accurately. Thus, although there are practically known terms in nonlinearities $h_{i,1}$, $h_{i,2}$, and $h_{i,3}$, we assume that $h_{i,1}$, $\bar{h}_{i,2}$, and $h_{i,3}$ are unknown.

Remark 1. Differential drive mobile robots considered in Atinç et al. (2013), Jin et al. (2015), Karkoub et al. (2019) and Poonawala et al. (2015) have the underactuated property in the kinematics because the position (x_i, y_i) and heading direction θ_i of the mobile robot are controlled by the linear and angular velocities. However, USVs have the underactuated property in the dynamics. In addition, as shown in the dynamics (3), the dynamics of USVs contains the sway velocity v_i, but the control inputs $\tau_{i,u}$ and $\tau_{i,r}$ do not exist in the sway dynamics. Thus, it is difficult to control the sway velocity using two control inputs $\tau_{i,u}$ and $\tau_{i,r}$. However, the differential drive mobile robots have linear and angular velocities in the kinematics and are fully actuated in their dynamics. Thus, the linear and angular velocities of the mobile robot can be controlled by two control torques of the dynamics. Due to these differences between kinematics and dynamics, the tracking control problem of USVs has been totally distinguished from that of differential drive mobile robots in the control community (see Do, 2011; Do & Pan, 2005; Park et al., 2017). Thus, the control laws presented in Atinç et al. (2013), Jin et al. (2015), Karkoub et al. (2019) and Poonawala et al. (2015) cannot be directly employed to the USV models (1) and (2).

Using (3), the leader–follower model using the relative distance l_{ij} and angle θ_{ij} between the leader j and the follower i is described by (Park & Yoo, 2019)

$$\begin{aligned}
\dot{l}_{ij} &= (-u_i + u_j)\cos(\psi_i - \theta_{ij}) + (\bar{v}_i - \bar{v}_j)\sin(\psi_j - \theta_{ij}), \\
\dot{\theta}_{ij} &= \frac{1}{l_{ij}}\{(-u_i + u_j)\sin(\psi_i - \theta_{ij}) \\
&\qquad - (\bar{v}_i - \bar{v}_j)\cos(\psi_i - \theta_{ij})\},
\end{aligned} \tag{4}$$

where $l_{ij} = \sqrt{(\bar{x}_j - \bar{x}_i)^2 + (\bar{y}_j - \bar{y}_i)^2}$ and $\theta_{ij} = \arctan 2(\bar{y}_j - \bar{y}_i, \bar{x}_j - \bar{x}_i)$.

Problem 1. Consider the kinematic and dynamic models of multiple uncertain USVs (3). Our problem is to design the control inputs $\tau_{i,u}$ and $\tau_{i,r}$ for each USV so that the desired formation is achieved while preserving connectivity and avoiding collisions with all other USVs and the obstacle, i.e.,

(i) Connectivity maintenance and collision avoidances: $R_{i,m} < l_{ij}(t) < L_i$, $\forall t \geq 0$,

(ii) Desired formation with predesignated performance: $\lim_{t\to\infty} |l_{ij}(t) - l_{ij,r}| < c_1$, $\lim_{t\to\infty} |\theta_{ij}(t) - \theta_{ij,r}| < c_2$,

(iii) Obstacle avoidance: $l_{i,b}(t) > R_{i,m}$, $\forall t \geq 0$,

where $R_{i,m}$ is the minimum avoidance range of the USV follower i, L_i is the minimum value of communication and sensing ranges

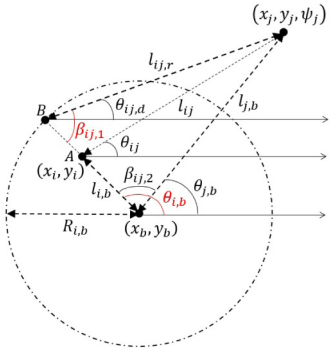

Fig. 1. Proposed obstacle avoidance strategy.

of the USV follower i, $l_{ij,r}$ and $\theta_{ij,r}$ denote the desired distance and angle between two USVs for achieving the desired formation, respectively, c_1 and c_2 are preselected positive constants, and $l_{i,b}$ is the distance between the USV follower i and the obstacle.

To deal with our formation control problem, the following assumptions and lemmas will be used for the formation control design and the stability analysis.

Assumption 1. The external disturbances $d_{i,n}$ are unknown and bounded as $|d_{i,n}| < \bar{d}_{i,n}$ where $n = 1, 2, 3$ and $\bar{d}_{i,n}$ are unknown constants.

Assumption 2. The nonlinear functions $h_{i,1}$, $h_{i,2}$, and $h_{i,3}$ in the dynamics (2) are unknown.

Assumption 3. The velocities u_j, $\bar{v}_j$, and r_j of the leader are bounded and unknown.

Assumption 4. The desired distance $l_{ij,r}$ and angle $\theta_{ij,r}$ are constants and bounded such that $R_{i,m} < l_{ij,r} < L_i$ and $-\pi/2 < \theta_{ij,r} < \pi/2$.

Lemma 1 (Bechlioulis & Rovithakis, 2014)**.** *Consider the initial value problem:*

$$\dot{\xi}(t) = h(t, \xi(t)), \quad \xi(t_0) \in \Omega_\xi \tag{5}$$

with $h : \mathcal{R}_+ \times \Omega_\xi \to \mathcal{R}^n$ where $\Omega_\xi \subset \mathcal{R}^n$ is a non-empty open set. Assume that h is: (a) locally Lipschitz on ξ, (b) continuous on t for each fixed $\xi \in \Omega_\xi$ and (c) locally integrable on t for each fixed $\xi \in \Omega_\xi$. Then, there exists a unique maximal solution $\xi : [t_0, t_{\max}) \to \Omega_\xi$ of (5) on the time interval $[t_0, t_{\max})$ with $t_{\max} \in \{\mathcal{R}^\star_+, \infty\}$ such that $\xi(t) \in \Omega_\xi$, $\forall t \in [t_0, t_{\max})$.

Lemma 2 (Bechlioulis & Rovithakis, 2014)**.** *Assume that the hypotheses of Lemma 1 hold. For a maximal solution $\xi : [t_0, t_{\max}) \to \Omega_\xi$ on the time interval $[t_0, t_{\max})$ with $t_{\max} < \infty$ and for any compact set $\Omega'_\xi \subset \Omega_\xi$, there exists a time instant $\bar{t} \in [t_0, t_{\max})$ such that $\xi(\bar{t}) \notin \Omega'_\xi$.*

3. Main result

In this section, we present a robust leader–follower formation control design for ensuring collision and obstacle avoidances and connectivity maintenance of multiple uncertain USVs with limited communication and sensing ranges. Connectivity-maintaining and collision-avoiding performance functions and the desired angle for the obstacle avoidance while preserving connectivity between the leader j and the follower i are derived to design novel nonlinear formation error functions.

3.1. Obstacle avoidance strategy while maintaining connectivity between USVs

Fig. 1 shows the proposed strategy to avoid the obstacle. In this figure, (x_b, y_b) is the position of the obstacle. To explain how to design the avoidance angle $\theta_{ij,d}$, let us assume that the USV is located on point A. Since $l_{i,b} < R_{i,b}$ where $R_{i,b}$ is the distance to start avoiding, the USV should do a maneuver for obstacle avoidance. Our strategy is to move the USV from point A to point B. Using the law of cosines, $\theta_{ij,d}$ can be represented by

$$\theta_{ij,d} = \beta_{ij,1} + \beta_{ij,2} - \pi + \theta_{j,b}. \tag{6}$$

where $\beta_{ij,1} = \arccos((l_{ij,r}^2 + R_{i,b}^2 - l_{j,b}^2)/(2l_{ij,r}R_{i,b}))$, $\beta_{ij,2} = \arccos((l_{j,b}^2 + R_{i,b}^2 - l_{ij,r}^2)/(2l_{j,b}R_{i,b}))$, and $l_{j,b}$ and $\theta_{j,b}$ denote the distance and the angle between the USV j and the obstacle, respectively. Thus, the USV will track $\theta_{ij,d}$ or $\theta_{ij,r}$ depending on the existence of the obstacle. However, this may cause the chattering phenomenon. To address this problem, we propose a continuous angle as follows:

$$\theta_{ij,d} = \begin{cases} \tanh\left(\frac{R_{i,b} - l_{i,b}}{\gamma_{ij,o1}}\right)\bar{\theta}_{ij,d} + \theta_{ij,r}, & l_{i,b} < R_{i,b}, \\ \theta_{ij,r}, & l_{i,b} \geq R_{i,b}, \end{cases} \tag{7}$$

where $\bar{\theta}_{ij,d} = \tanh\left(\frac{\theta_{j,b} - \psi_j}{\gamma_{ij,o2}}\right)(\beta_{ij,1} + \beta_{ij,2} - \pi) + \theta_{j,b} - \theta_{ij,r}$; $\gamma_{ij,o1} > 0$ and $\gamma_{ij,o2} > 0$ are constants.

Remark 2. If we remove the terms $\tanh\left(\frac{R_{i,b} - l_{i,b}}{\gamma_{ij,o1}}\right)$ and $\tanh\left(\frac{\theta_{j,b} - \psi_j}{\gamma_{ij,o2}}\right)$ in (7), then (7) becomes

$$\theta_{ij,d} = \begin{cases} \beta_{ij,1} + \beta_{ij,2} - \pi + \theta_{j,b}, & l_{i,b} < R_{i,b}, \\ \theta_{ij,r}, & l_{i,b} \geq R_{i,b}. \end{cases}$$

This equation means that the desired angle $\theta_{ij,d}$ is switched by the distance $l_{i,b}$ between the USV i and the obstacle for collision avoidance and formation tracking. However, the switching of desired angle $\theta_{ij,d}$ can cause the oscillation. Thus, we use $\tanh\left(\frac{R_{i,b} - l_{i,b}}{\gamma_{ij,o1}}\right)$ to make a continuous angle. Additionally, $\tanh\left(\frac{\theta_{j,b} - \psi_j}{\gamma_{ij,o2}}\right)$ is used to ensure collision avoidance in all positions between the leader and the follower.

Notice that the USV i can easily calculate $l_{j,b}$ and $\theta_{j,b}$ in (7) without transmitting data from the USV j using the following equations

$$l_{j,b} = \sqrt{a_{ij}^2 + b_{ij}^2}, \quad \theta_{j,b} = \arctan\left(\frac{a_{ij}}{b_{ij}}\right). \tag{8}$$

where $a_{ij} = l_{ij}\sin\theta_{ij} + l_{i,b}\sin\theta_{i,b}$ and $b_{ij} = l_{ij}\cos\theta_{ij} + l_{i,b}\cos\theta_{i,b}$.

Remark 3. To preserve connectivity during the obstacle avoidance, we propose an obstacle avoidance strategy by designing the avoidance angle $\theta_{ij,d}$ while fixing the avoidance distance as $l_{ij,r}$. If the desired distance between the USVs i and j changes while avoiding the obstacle, then it is difficult to preserve connectivity between USVs i and j because the distance between the USVs i and j can be larger than L_i due to the increase of the formation errors during the obstacle avoidance. Thus, we set the desired distance during the obstacle avoidance to $l_{ij,r}$.

3.2. Leader–follower formation control design using connectivity-maintaining and collision-avoiding performance functions

Let us define the formation and velocity errors as

$$e_{ij,1} = l_{ij} - l_{ij,r}, \tag{9}$$

$$e_{ij,2} = \theta_{ij} - \bar{\theta}_{ij,d}, \tag{10}$$

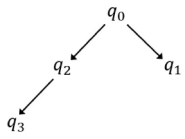

Fig. 2. The initial connectivity of multiple USVs.

$$e_{ij,3} = \psi_i - \bar{\psi}_{ij,a}, \tag{11}$$
$$e_{i,4} = u_i - u_{i,v}, \tag{12}$$
$$e_{i,5} = \bar{v}_i - v_{i,v} - \tanh \eta_i, \tag{13}$$
$$e_{i,6} = r_i - r_{i,v}, \tag{14}$$

where $\bar{\theta}_{ij,d}$ and $\bar{\psi}_{ij,a}$ denote the signals filtered by $\gamma_{ij,\theta}\dot{\bar{\theta}}_{ij,d} + \bar{\theta}_{ij,d} = \theta_{ij,d}$ with $\bar{\theta}_{ij,d}(t_0) = \theta_{ij,d}(t_0)$ and a constant $\gamma_{ij,\theta} > 0$, and $\gamma_{ij,\psi}\dot{\bar{\psi}}_{ij,a} + \bar{\psi}_{ij,a} = \psi_{ij,a}$ with $\bar{\psi}_{ij,a}(t_0) = \psi_{ij,a}(t_0)$ and a constant $\gamma_{ij,\psi} > 0$, respectively. $u_{i,v}$, $v_{i,v}$, and $r_{i,v}$ are virtual controls, and η_i is an auxiliary signal to deal with the underactuated problem. Here, $\psi_{ij,a}$ is an approach angle defined as $\psi_{ij,a} = \{\arctan 2(f_{ij,1}, f_{ij,2}) - \psi_j\}\tanh(f_{ij,3}) + \psi_j$ where $f_{ij,1} = l_{ij}\sin\theta_{ij} - l_{ij,r}\sin\bar{\theta}_{ij,d}$, $f_{ij,2} = l_{ij}\cos\theta_{ij} - l_{ij,r}\cos\bar{\theta}_{ij,d}$, and $f_{ij,3} = \{(l_{ij,r} - l_{ij})^2 + (\bar{\theta}_{ij,d} - \theta_{ij})^2\}/\gamma_{ij,a}$ with a constant $\gamma_{ij,a} > 0$

Remark 4. (i) In (10) and (11), the filtered signals $\bar{\theta}_{ij,d}$ and $\bar{\psi}_{ij,a}$ are used instead of $\theta_{ij,d}$ and $\psi_{ij,a}$, respectively, to avoid the requirement of the velocity information of the USVs in the formation control design procedure.

(ii) The approach angle $\psi_{ij,a}$ is essential for the tracking control of the USVs because there is no control input in the sway dynamics (3). If the heading angle ψ_j is used instead of $\psi_{ij,a}$ in (11), then the position errors cannot be reduced when the orientation error goes to zero. Thus, the error (11) using the approach angle $\psi_{ij,a}$ is designed.

(iii) In Chaw (2011) and Peng et al. (2013), since the boundedness of the sway velocity v_i may not be proved theoretically due to the lack of the control input, it is assumed that the sway velocity is passive-bounded. To remove this assumption, we employ the auxiliary signal η_i in (13) for the stability analysis of the sway dynamics.

To design the predesignated-performance-based formation controller guaranteeing the connectivity preservation and the collision avoidance between USV i and USV j, let us normalize the formation and velocity errors in (9)–(14) as

$$z_{ij,1} = \frac{2e_{ij,1} - \rho^U_{ij,1} + \rho^L_{ij,1}}{\rho^U_{ij,1} + \rho^L_{ij,1}}, \tag{15}$$
$$z_{ij,n} = \frac{e_{ij,n}}{\rho_{ij,n}},\ n = 2, 3, \quad z_{i,p} = \frac{e_{i,p}}{\rho_{i,p}},\ p = 4, 5, 6 \tag{16}$$

where $\rho^U_{ij,1}$ and $\rho^L_{ij,1}$ denote connectivity-maintaining and collision-avoiding performance functions, $\rho_{ij,n}$ and $\rho_{i,p}$ are the performance functions for the approximation-free formation tracker design, and they are defined as

$$\rho^U_{ij,1} = \{\rho^U_{ij,1}(t_0) - \rho^U_{ij,1}(\infty)\}e^{-\mu_{ij,1}t} + \rho^U_{ij,1}(\infty), \tag{17}$$
$$\rho^L_{ij,1} = \{\rho^L_{ij,1}(t_0) - \rho^L_{ij,1}(\infty)\}e^{-\mu_{ij,1}t} + \rho^L_{ij,1}(\infty), \tag{18}$$
$$\rho_{ij,n} = \{\rho_{ij,n}(t_0) - \rho_{ij,n}(\infty)\}e^{-\mu_{ij,n}t} + \rho_{ij,n}(\infty), \tag{19}$$
$$\rho_{i,p} = \{\rho_{i,p}(t_0) - \rho_{i,p}(\infty)\}e^{-\mu_{i,p}t} + \rho_{i,p}(\infty). \tag{20}$$

In these expressions, t_0 represents the initial time, $\mu_{ij,1}$, $\mu_{ij,n}$, and $\mu_{i,p}$ are positive constants; $\rho^U_{ij,1}$, $\rho^L_{ij,1}$, $\rho_{ij,n}$, and $\rho_{i,p}$ are chosen to satisfy

$$\begin{aligned}
&0 < \rho^U_{ij,1}(\infty) < \rho^U_{ij,1}(t_0) \le L_i - l_{ij,r},\\
&-\rho^L_{ij,1}(t_0) < e_{ij,1}(t_0) < \rho^U_{ij,1}(t_0),\\
&0 < \rho^L_{ij,1}(\infty) < \rho^L_{ij,1}(t_0) \le l_{ij,r} - R_{i,m},\\
&0 < \rho_{ij,2}(\infty) < \rho_{ij,2}(t_0) = \pi,\\
&|e_{ij,n}(t_0)| < \rho_{ij,n}(t_0),
\end{aligned} \tag{21}$$
$$|e_{i,p}(t_0)| < \rho_{i,p}(t_0). \tag{22}$$

Using (15) and (16), the leader–follower formation control scheme for the USV follower i is designed as follows:

$$u_{i,v} = k_{i,1}\varepsilon_{i,1}\cos(\psi_i - \theta_{ij}) + k_{i,2}\varepsilon_{i,2}\sin(\psi_i - \theta_{ij}), \tag{23}$$
$$v_{i,v} = -k_{i,1}\varepsilon_{i,1}\sin(\psi_i - \theta_{ij}) + k_{i,2}\varepsilon_{i,2}\cos(\psi_i - \theta_{ij}), \tag{24}$$
$$r_{i,v} = -k_{i,3}\varepsilon_{i,3}, \tag{25}$$
$$\tau_{i,u} = -k_{i,4}\varepsilon_{i,4}, \tag{26}$$
$$\tau_{i,r} = -k_{i,6}\varepsilon_{i,6}, \tag{27}$$
$$\dot{\eta}_i = k_{i,5}\varepsilon_{i,5}\cosh^2\eta_i - \lambda_i\sinh\eta_i\cosh\eta_i, \tag{28}$$

where $k_{i,\nu} > 0$, $\nu = 1, \ldots, 6$, $\lambda_i > 0$ are design parameters, $\varepsilon_{i,n} = \ln\left(\frac{1+z_{ij,n}}{1-z_{ij,n}}\right)$, $n = 1, 2, 3$, $\varepsilon_{i,p} = \ln\left(\frac{1+z_{i,p}}{1-z_{i,p}}\right)$, $p = 4, 5, 6$, and $\eta_i(t_0) = 0$.

Remark 5. The proposed leader–follower formation error (15) is based on the performance functions $\rho^U_{ij,1}$ and $\rho^L_{ij,1}$ for ensuring collision avoidance and connectivity preservation, respectively. The error surfaces (16) with the performance functions (19) and (20) are defined to achieve the approximation-free control design in the predesignated-performance-based control sense (Bechlioulis & Rovithakis, 2014). In (23)–(28), $\varepsilon_{i,\nu}$, $\nu = 1, \ldots, 6$ are used as nonlinear error surfaces for the formation control design. If $\varepsilon_{i,\nu}$ is bounded, $|z_{ij,n}| < 1$ and $|z_{i,p}| < 1$ are ensured where $n = 1, 2, 3$ and $p = 4, 5, 6$. Especially, from (15), $|z_{ij,1}| < 1$ implies $-\rho^L_{ij,1} < e_{ij,1} < \rho^U_{ij,1}$. The conditions in (21) yield $R_{i,m} < l_{ij} < L_i$. Thus, the boundedness of $\varepsilon_{i,1}$ ensures collision avoidance and connectivity preservation while achieving the desired formation. We will prove the boundedness of $\varepsilon_{i,\nu}$ by using the proposed control laws (23)–(28) in Theorem 1.

Theorem 1. *Consider the multiple uncertain USVs (3) controlled by the proposed leader–follower formation control schemes (23)–(28). Under Assumptions 1–4, the following results hold:*

(1) The connectivity preservation and the collision avoidance between the USV follower i and USV leader j are guaranteed, i.e., $R_{i,m} < l_{ij}(t) < L_i$, $\forall t \ge t_0$. Moreover, the bounds of the formation errors can be adjustable by the choice of the predefined performance functions, i.e., $\lim_{t\to\infty}|l_{ij}(t) - l_{ij,r}| < \max\{\rho^L_{ij,1}(\infty), \rho^U_{ij,1}(\infty)\}$ and $\lim_{t\to\infty}|\theta_{ij}(t) - \theta_{ij,r}| < \rho_{ij,2}(\infty)$.

(2) If $R_{i,b}$ is chosen to satisfy that $R_{i,b} = l_{i,a} + R_{i,m} + \gamma_{i,b}$ where $\gamma_{i,b}$ is a positive constant and $l_{i,a} = \sqrt{l^2_{ij,r} + (l_{ij,r} + \rho^U_{ij,1}) - 2l_{ij,r}(l_{ij,r} - \rho^L_{ij,1})\cos\rho_{ij,2}}$, the collision avoidance with the obstacle is guaranteed, i.e., $R_{i,m} < l_{i,b}(t)$, $\forall t \ge t_0$.

Proof. Differentiating (15) and (16) with respect to time, and employing (3), (4), and (9)–(14), we have

$$\begin{aligned}
\dot{z}_{ij,1} &= s_{ij,1}(t, z_{ij,1}, z_{ij,2}, z_{i,4}, z_{i,5}, z_{j,4}, z_{j,5})\\
&= \frac{-2u_{i,v}\cos(\psi_i - \theta_{ij}) + 2v_{i,v}\sin(\psi_i - \theta_{ij}) + 2g_{ij,1}}{\rho^U_{ij,1} + \rho^L_{ij,1}},
\end{aligned} \tag{29}$$

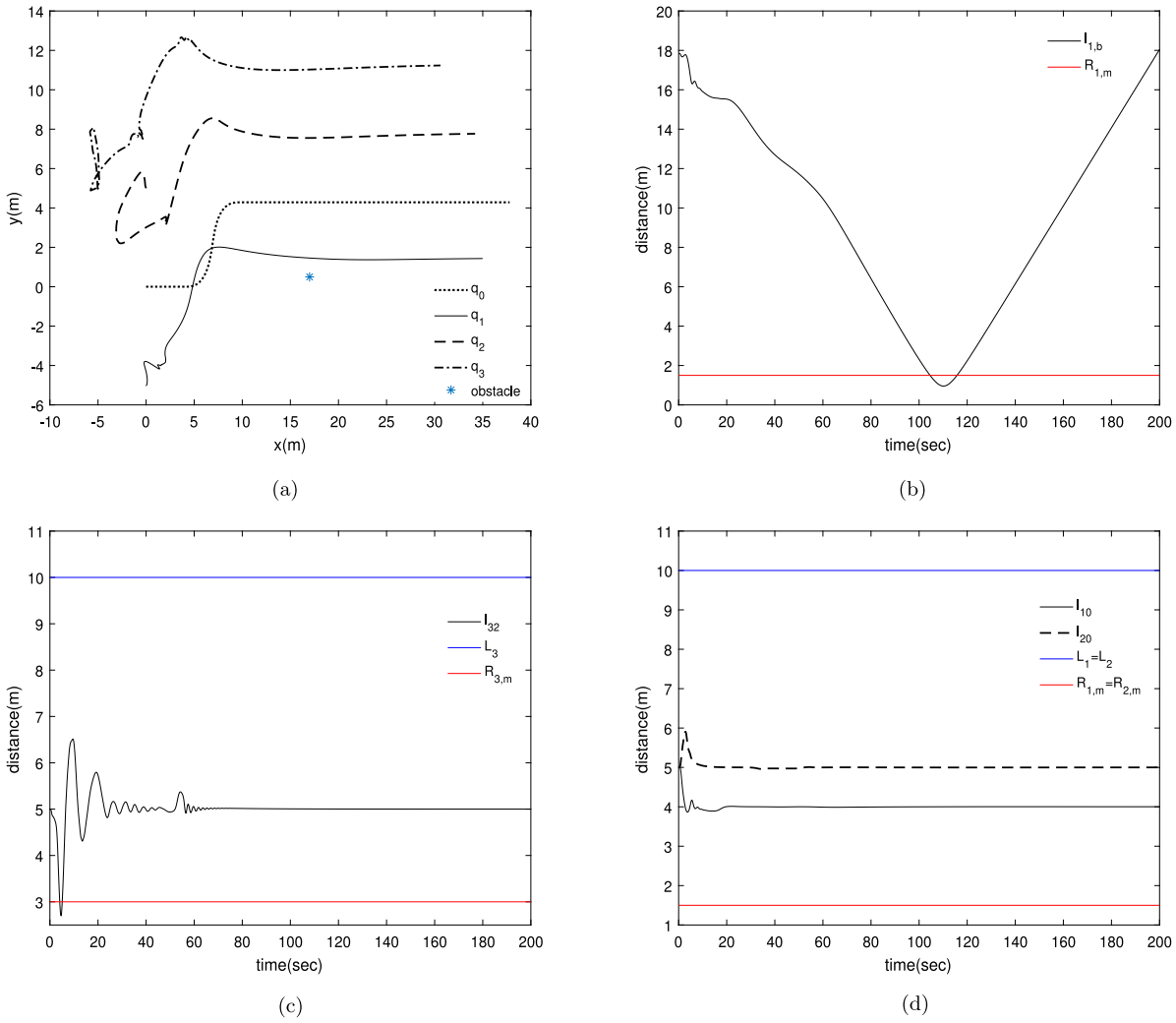

Fig. 3. Simulation results for Case 1 (a) formation tracking result (b) $l_{1,b}$ (c) l_{32} (d) l_{10} and l_{20}.

$$\dot{z}_{ij,2} = s_{ij,2}(t, z_{ij,1}, z_{ij,2}, z_{i,4}, z_{i,5}, z_{j,4}, z_{j,5}) = \frac{-u_{i,v}\sin(\psi_i - \theta_{ij}) - v_{i,v}\cos(\psi_i - \theta_{ij}) + g_{ij,2}}{l_{ij}\rho_{ij,2}}, \tag{30}$$

$$\dot{z}_{ij,3} = s_{ij,3}(t, z_{ij,3}, z_{i,6}) = \frac{r_{i,v} + g_{ij,3}}{\rho_{ij,3}}, \tag{31}$$

$$\dot{z}_{i,4} = s_{i,4}(t, z_{ij,1}, z_{ij,2}, z_{ij,3}, z_{i,4}, z_{i,5}, z_{i,6}) = \frac{\tau_{i,u}/m_{i,11} + g_{i,4}}{\rho_{i,4}}, \tag{32}$$

$$\dot{z}_{i,5} = s_{i,5}(t, z_{ij,1}, z_{ij,2}, z_{ij,3}, z_{i,4}, z_{i,5}, z_{i,6}) = \frac{-\dot{\eta}_i/\cosh^2\eta_i + g_{i,5}}{\rho_{i,5}}, \tag{33}$$

$$\dot{z}_{i,6} = s_{i,6}(t, z_{ij,1}, z_{ij,2}, z_{ij,3}, z_{i,4}, z_{i,5}, z_{i,6}) = \frac{m_{i,22}\tau_{i,r}/\Delta_i + g_{i,6}}{\rho_{i,6}}, \tag{34}$$

where

$$\begin{aligned} g_{ij,1} =& -z_{i,4}\rho_{i,4}\cos(\psi_i - \theta_{ij}) \\ &+ (z_{i,5}\rho_{i,5} + \tanh\eta_i)\sin(\psi_i - \theta_{ij}) \\ &+ u_j\cos(\psi_j - \theta_{ij}) - \bar{v}_j\sin(\psi_j - \theta_{ij}) \\ &- \frac{1}{2}(\dot{\rho}^U_{ij,1} - \dot{\rho}^L_{ij,1} + z_{ij,1}(\dot{\rho}^U_{ij,1} + \dot{\rho}^L_{ij,1})), \end{aligned}$$

$$\begin{aligned} g_{ij,2} =& -z_{i,4}\rho_{i,4}\sin(\psi_i - \theta_{ij}) \\ &- (z_{i,5}\rho_{i,5} + \tanh\eta_i)\cos(\psi_i - \theta_{ij}) \\ &+ u_j\sin(\psi_j - \theta_{ij}) + \bar{v}_j\cos(\psi_j - \theta_{ij}) \\ &- l_{ij}\dot{\bar{\theta}}_{ij,d} - l_{ij}z_{ij,2}\dot{\rho}_{ij,2}, \end{aligned}$$

$$g_{ij,3} = z_{i,6}\rho_{i,6} - \dot{\bar{\psi}}_{ij,a} - z_{ij,3}\dot{\rho}_{ij,3},$$

$$\begin{aligned} g_{i,4} =& h_{i,1}(z_{i,4}\rho_{i,4} + u_{i,v}, z_{i,5}\rho_{i,5} + v_{i,v} + \tanh\eta_i, \\ & z_{i,6}\rho_{i,6} + r_{i,v}) + d_{i,1} - \dot{u}_{i,v} - z_{i,4}\dot{\rho}_{i,4}, \end{aligned}$$

$$\begin{aligned} g_{i,5} =& \bar{h}_{i,2}(z_{i,4}\rho_{i,4} + u_{i,v}, z_{i,5}\rho_{i,5} + v_{i,v} + \tanh\eta_i, \\ & z_{i,6}\rho_{i,6} + r_{i,v}) + \bar{d}_{i,2} - \dot{v}_{i,v} - z_{i,5}\dot{\rho}_{i,5}, \end{aligned}$$

$$\begin{aligned} g_{i,6} =& h_{i,3}(z_{i,4}\rho_{i,4} + u_{i,v}, z_{i,5}\rho_{i,5} + v_{i,v} + \tanh\eta_i, \\ & z_{i,6}\rho_{i,6} + r_{i,v}) + d_{i,3} - \dot{r}_{i,v} - z_{i,6}\dot{\rho}_{i,6}. \end{aligned}$$

Define the nonempty and open set $\Omega_m = (-1, 1)$ where $m = 1, \ldots, 6$. Since the initial values of the performance functions are selected to be $|z_{ij,n}(t_0)| < 1$ and $|z_{i,p}(t_0)| < 1$ in (21) and (22), $z_{ij,n}(t_0) \in \Omega_n$ and $z_{i,p}(t_0) \in \Omega_p$ where $n = 1, 2, 3$ and $p = 4, 5, 6$. From Assumption 4 and (8), $\theta_{ij,d}$ in (7) is bounded. In addition, $\psi_{ij,a}$ is bounded from its definition. Then, because $\bar{\theta}_{ij,d}$ and $\bar{\psi}_{ij,a}$ are low pass filtered signals of the bounded signals $\theta_{ij,d}$ and $\psi_{ij,a}$, respectively, $\bar{\theta}_{ij,d}$ and $\bar{\psi}_{ij,a}$ are also bounded. From $\dot{\bar{\theta}}_{ij,d} = (\theta_{ij,d} - \bar{\theta}_{ij,d})/\gamma_{ij,\theta}$ and $\dot{\bar{\psi}}_{ij,a} = (\psi_{ij,a} - \bar{\psi}_{ij,a})/\gamma_{ij,\psi}$, the boundedness of $\theta_{ij,d}$, $\psi_{ij,a}$, $\bar{\theta}_{ij,d}$, and $\bar{\psi}_{ij,a}$ implies that $\dot{\bar{\theta}}_{ij,d}$ and $\dot{\bar{\psi}}_{ij,a}$ are bounded.

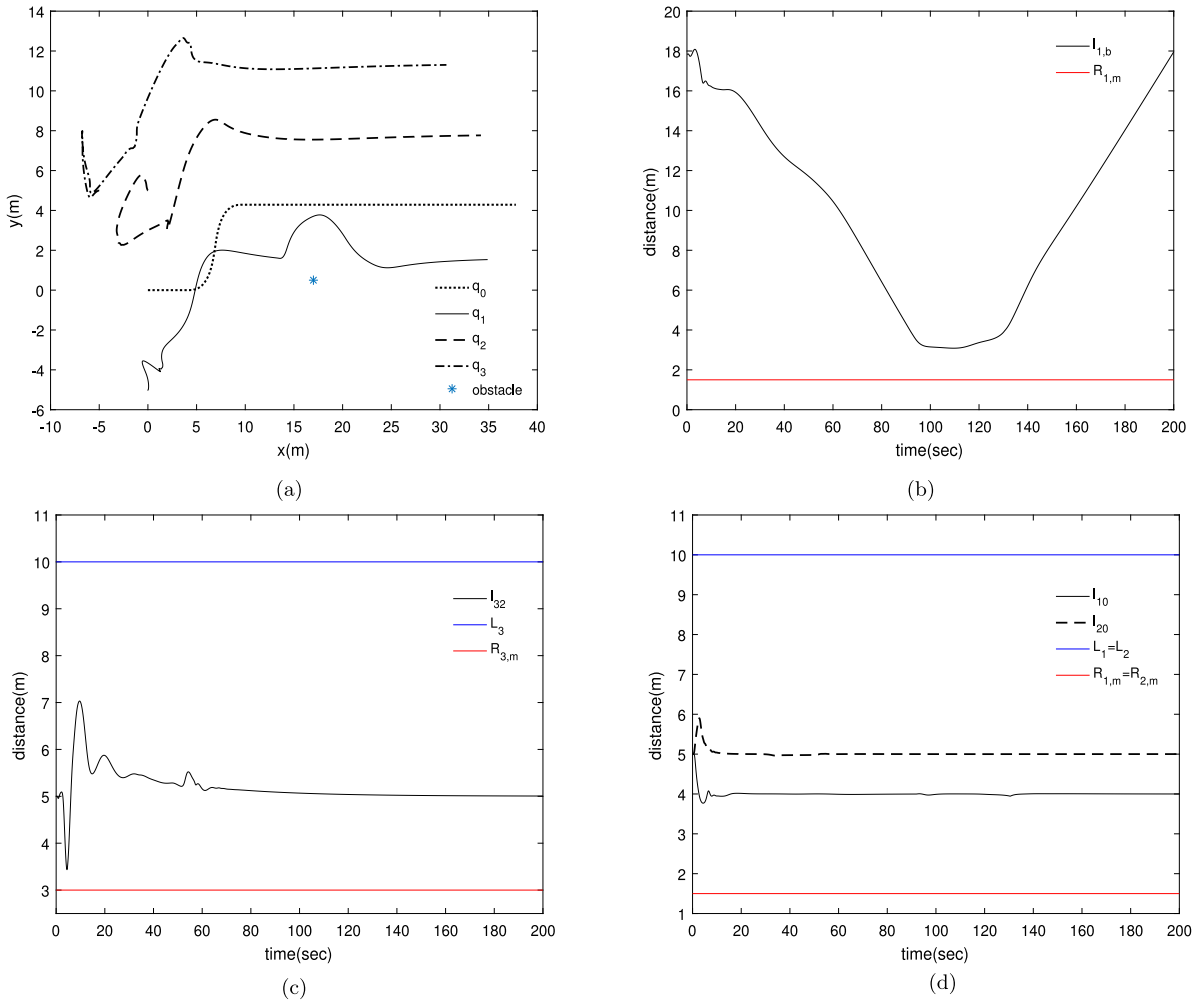

Fig. 4. Simulation results for Case 2 (a) formation tracking result (b) $l_{1,b}$ (c) l_{32} (d) l_{10} and l_{20}.

Thus, under Assumptions 1–4, $s_{ij,n}$ and $s_{i,p}$ are locally Lipschitz on $z_{ij,n}$ and $z_{i,p}$, respectively, and continuously differentiable on t for $z_{ij,n} \in \Omega_n$ and $z_{i,p} \in \Omega_p$. Therefore, from Lemma 1, there exist maximal solutions $z_{ij,n}(t)$ and $z_{i,p}(t)$ satisfying $z_{ij,n}(t) \in \Omega_n$ and $z_{i,p}(t) \in \Omega_p$, $\forall t \in [t_0, t_{\max})$.

For the proof, the following steps are given.

Step 1: Consider the positive definite and radially unbounded function $V_{i,1}(t) = \frac{1}{2}\sum_{n=1}^{3} \varepsilon_{i,n}^2(t)$ for all $t \in [t_0, t_{\max})$. From (29)–(23) and (31)–(25), the time derivatives of $\varepsilon_{i,n}$ are represented by

$$\begin{aligned}
\dot{\varepsilon}_{i,1} &= \frac{4}{(1-z_{ij,1}^2)(\rho_{ij,1}^U + \rho_{ij,1}^L)}\{-k_{i,1}\varepsilon_{i,1} + g_{ij,1}\},\\
\dot{\varepsilon}_{i,2} &= \frac{2}{(1-z_{ij,2}^2)\rho_{ij,2} l_{ij}}\{-k_{i,2}\varepsilon_{i,2} + g_{ij,2}\},\\
\dot{\varepsilon}_{i,3} &= \frac{2}{(1-z_{ij,3}^2)\rho_{ij,3}}\{-k_{i,3}\varepsilon_{i,3} + g_{ij,3}\}.
\end{aligned} \tag{35}$$

From $z_{ij,n}(t) \in \Omega_n$ and $z_{i,p}(t) \in \Omega_p$, $\forall t \in [t_0, t_{\max})$, the boundedness of the performance functions (17)–(20) and their time derivatives, and Assumption 3, there exist unknown constants $\delta_{i,1}$, $\delta_{i,2}$, and $\delta_{i,3}$ satisfying

$$|g_{ij,1}(t)| \le \delta_{i,1}, \ \ |g_{ij,2}(t)| \le \delta_{i,2}, \ \ |g_{ij,3}(t)| \le \delta_{i,3}, \tag{36}$$

for all $t \in [t_0, t_{\max})$. Using (35) and (36), the time derivative of $\dot{V}_{i,1}$ becomes

$$\begin{aligned}
\dot{V}_{i,1} \le & \frac{4}{(1-z_{ij,1}^2)(\rho_{ij,1}^U + \rho_{ij,1}^L)}\{-k_{i,1}|\varepsilon_{i,1}|^2 + \delta_{i,1}|\varepsilon_{i,1}|\}\\
& + \frac{2}{(1-z_{ij,2}^2)\rho_{ij,2} l_{ij}}\{-k_{i,2}|\varepsilon_{i,2}|^2 + \delta_{i,2}|\varepsilon_{i,2}|\}\\
& + \frac{2}{(1-z_{ij,3}^2)\rho_{ij,3}}\{-k_{i,3}|\varepsilon_{i,3}|^2 + \delta_{i,3}|\varepsilon_{i,3}|\},
\end{aligned} \tag{37}$$

for all $t \in [t_0, t_{\max})$. Owing to $z_{ij,n}(t) \in \Omega_n$ and $z_{i,p}(t) \in \Omega_p$, $\forall t \in [t_0, t_{\max})$, it holds that $4/((1-z_{ij,1}^2)(\rho_{ij,1}^U + \rho_{ij,1}^L)) > 0$, $2/((1-z_{ij,2}^2)\rho_{ij,2} l_{ij}) > 0$, and $2/((1-z_{ij,3}^2)\rho_{ij,3}) > 0$. Thus, (37) implies that $\dot{V}_{i,1}$ is negative when $|\varepsilon_{i,n}| > \delta_{i,n}/k_{i,n}$, $n = 1, 2, 3$. This means that $\varepsilon_{i,n}$ are bounded as $|\varepsilon_{i,n}(t)| \le \bar{\varepsilon}_{i,n} = \max\{|\varepsilon_{i,n}(t_0)|, \frac{\delta_{i,n}}{k_{i,n}}\}$ for all $t \in [t_0, t_{\max})$. Thus, the virtual controls $u_{i,v}(t)$, $v_{i,v}(t)$, and $r_{i,v}(t)$ remain bounded for all $t \in [t_0, t_{\max})$. From (35), it leads to the boundedness of $\dot{u}_{i,v}(t)$, $\dot{v}_{i,v}(t)$, and $\dot{r}_{i,v}(t)$ for all $t \in [t_0, t_{\max})$.

Step 2: Consider the positive definite and radially unbounded function

$$V_{i,2}(t) = \frac{1}{2}\left(m_{i,11}\varepsilon_{i,4}^2(t) + \varepsilon_{i,5}^2(t) + \frac{\Delta_i}{m_{i,22}}\varepsilon_{i,6}^2(t)\right) \tag{38}$$

for all $t \in [t_0, t_{\max})$.

By Assumptions 1–4, $z_{i,p}(t) \in \Omega_p$, $p = 4, 5, 6$, $\forall t \in [t_0, t_{\max})$, and the results of Step 1, there exist unknown positive constants

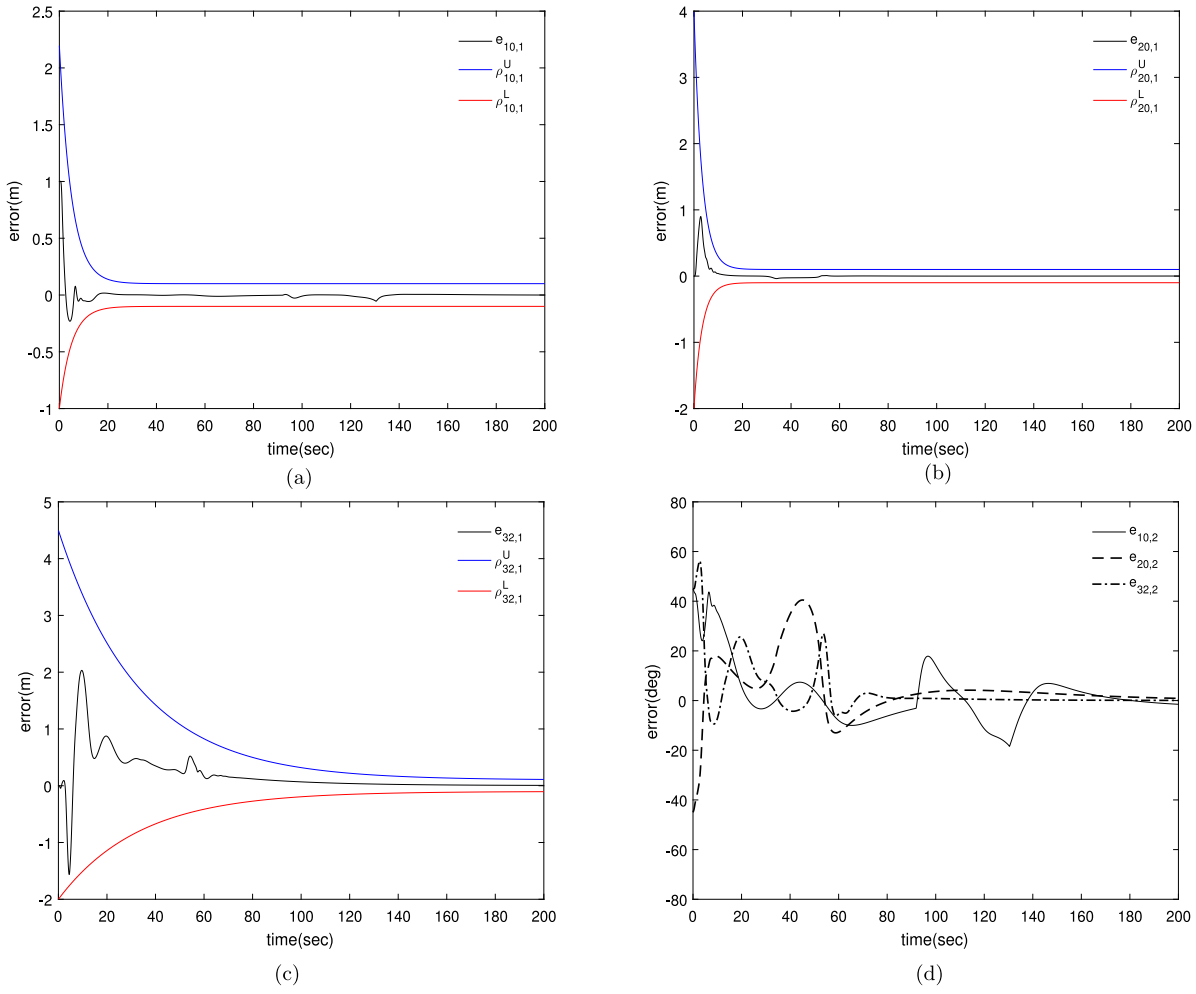

Fig. 5. Formation tracking errors for Case 2 (a) $e_{10,1}$, $\rho^U_{10,1}$, $\rho^L_{10,1}$ (b) $e_{20,1}$, $\rho^U_{20,1}$, $\rho^L_{20,1}$ (c) $e_{32,1}$, $\rho^U_{32,1}$, $\rho^L_{32,1}$ (d) desired angle errors.

$\delta_{i,4}$, $\delta_{i,5}$, and $\delta_{i,6}$ satisfying

$$|m_{i,11}g_{i,4}| \le \delta_{i,4},$$
$$|g_{i,5} + \lambda_i \tanh \eta_i| \le \delta_{i,5}, \quad \left|\frac{\Delta_i}{m_{i,22}} g_{i,6}\right| \le \delta_{i,6}. \tag{39}$$

Using (32)–(34), (26)–(28), and (39), the time derivative of (38) becomes

$$\begin{aligned}\dot{V}_{i,2} \le & \frac{2}{(1-z_{i,4}^2)\rho_{i,4}}\{-k_{i,4}|\varepsilon_{i,4}|^2 + \delta_{i,4}|\varepsilon_{i,4}|\} \\ & + \frac{2}{(1-z_{i,5}^2)\rho_{i,4}}\{-k_{i,5}|\varepsilon_{i,5}|^2 + \delta_{i,5}|\varepsilon_{i,5}|\} \\ & + \frac{2}{(1-z_{i,6}^2)\rho_{i,6}}\{-k_{i,6}|\varepsilon_{i,6}|^2 + \delta_{i,6}|\varepsilon_{i,6}|\},\end{aligned} \tag{40}$$

for all $t \in [t_0, t_{\max})$. Similar to Step 1, one can show the boundedness of $\varepsilon_{i,p}$, $p = 4, 5, 6$, such that $|\varepsilon_{i,p}(t)| \le \bar{\varepsilon}_{i,p} = \max\{|\varepsilon_{i,p}(t_0)|, \delta_{i,p}/k_{i,p}\}$ for all $t \in [t_0, t_{\max})$.

From Steps 1 and 2, using the boundedness of $\varepsilon_{i,\nu}$, $\nu = 1, \ldots, 6$, gives

$$-1 < \frac{e^{-\bar{\varepsilon}_{i,n}} - 1}{e^{-\bar{\varepsilon}_{i,n}} + 1} = \underline{z}_{ij,n} \le z_{ij,n} \le \bar{z}_{ij,n} = \frac{e^{\bar{\varepsilon}_{i,n}} - 1}{e^{\bar{\varepsilon}_{i,n}} + 1} < 1, \tag{41}$$

$$-1 < \frac{e^{-\bar{\varepsilon}_{i,p}} - 1}{e^{-\bar{\varepsilon}_{i,p}} + 1} = \underline{z}_{i,p} \le z_{i,p} \le \bar{z}_{i,p} = \frac{e^{\bar{\varepsilon}_{i,p}} - 1}{e^{\bar{\varepsilon}_{i,p}} + 1} < 1, \tag{42}$$

where $n = 1, 2, 3$ and $p = 4, 5, 6$. Note that (41) and (42) imply $z_{ij,n}(t) \in \Omega'_{i,n} \subset \Omega_{i,n}$ and $z_{i,p} \in \Omega'_{i,p} \subset \Omega_{i,p}$, $\forall t \in [t_0, t_{\max})$, respectively, where $\Omega'_{i,n} = [\underline{z}_{ij,n}, \bar{z}_{ij,n}]$ and $\Omega'_{i,p} = [\underline{z}_{i,p}, \bar{z}_{i,p}]$. Then, Lemma 2 indicates the existence of $\bar{t} \in [t_0, t_{\max})$ with $t_{\max} < \infty$ such that $z_{ij,n}(\bar{t}) \notin \Omega'_{i,n}$ and $z_{i,p}(\bar{t}) \notin \Omega'_{i,p}$. Since this is a contradiction, $t_{\max} = \infty$.

Proof of (1): Using the boundedness of $\varepsilon_{i,1}(t)$, $\forall t \ge t_0$, and (15), we obtain

$$-\rho^L_{ij,1} < e_{ij,1}(t) < \rho^U_{ij,1}, \quad \forall t \ge t_0. \tag{43}$$

Using (9) and (21), we can rewrite (43) as $R_{i,m} < l_{ij}(t) < L_i$, $\forall t \ge t_0$. Therefore, the connectivity maintenance and the collision avoidance of the USV i and USV j are guaranteed for all $t \ge t_0$. Moreover, from (43), we can also obtain

$$\begin{aligned}& -\rho^L_{ij,1}(\infty) < e_{ij,1}(\infty) < \rho^U_{ij,1}(\infty), \\ & \therefore \lim_{t\to\infty} |l_{ij}(t) - l_{ij,r}| < \max\{\rho^L_{ij,1}(\infty), \rho^U_{ij,1}(\infty)\}.\end{aligned} \tag{44}$$

If there is no collision, $\bar{\theta}_{ij,d} = \theta_{ij,r}$ in (7). Using this fact, it is similarly deduced that $\lim_{t\to\infty} |\theta_{ij}(t) - \theta_{ij,r}| < \rho_{ij,2}(\infty)$. Therefore, the formation errors are bounded and can be adjustable by the choice of $\rho^L_{ij,1}(\infty)$, $\rho^U_{ij,1}(\infty)$, and $\rho_{ij,2}(\infty)$. This completes the proof of Theorem 1-(1).

Proof of (2): Since $|\theta_{ij} - \theta_{ij,d}| < \rho_{ij,2} \le \pi$, it holds from Fig. 1 that

$$R_{i,b} - l_{i,b} = \sqrt{l_{ij,r}^2 + l_{ij}^2 - 2l_{ij,r}l_{ij}\cos(\theta_{ij} - \theta_{ij,d})} < l_{i,a}.$$

This induces $l_{i,b} > R_{i,b} - l_{i,a}$. Therefore, if $R_{i,b}$ is chosen to satisfy that $R_{i,b} = l_{i,a} + R_{i,m} + \gamma_{i,b}$, then $l_{i,b} > R_{i,m}$, $\forall t \ge t_0$. This means that

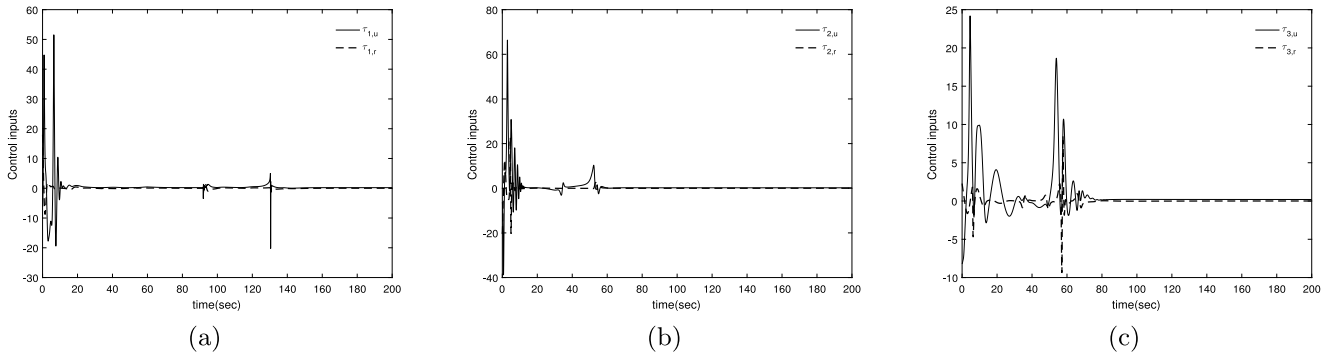

Fig. 6. Control inputs for Case 2 (a) $\tau_{1,u}$ (N) and $\tau_{1,r}$ (N m) (b) $\tau_{2,u}$ (N) and $\tau_{2,r}$ (N m) (c) $\tau_{3,u}$ (N) and $\tau_{3,r}$ (N m).

the obstacle avoidance is guaranteed for all $t \geq t_0$. This completes the proof of (2). ■

Remark 6. The performance functions and design parameters for the connectivity maintenance and collision avoidance are chosen as the following steps: (i) select $\rho^U_{ij,1}$ and $\rho^L_{ij,1}$ to satisfy (21) according to the given L_i, $l_{ij,r}$, $R_{i,m}$, and $e_{ij,1}(t_0)$. (ii) Select $\rho_{ij,2}$ and $\rho_{ij,3}$ by the conditions of (22), respectively. (iii) Choose $\gamma_{i,b}$ for $R_{i,b}$. (iv) After choosing $k_{i,1} > 0$, $k_{i,2} > 0$, and $k_{i,3} > 0$, calculate $e_{i,4}(t_0)$, $e_{i,5}(t_0)$, and $e_{i,6}(t_0)$ using (12)–(14) and (23)–(25). (v) According to $e_{i,4}(t_0)$, $e_{i,5}(t_0)$, and $e_{i,6}(t_0)$, choose $\rho_{i,4}$, $\rho_{i,5}$, and $\rho_{i,6}$.

4. Simulation results

In this section, we consider four USVs with the communication link shown in Fig. 2 and use the model parameters of the USVs given in Skjetne et al. (2005). In Fig. 2, the global leader is the USV 0 and its position is defined as q_0. The limited communication and sensing range is defined as $L_i = 10$ where $i = 1, 2, 3$. The design parameters are chosen as $k_{n,1} = 10$, $k_{p,1} = 5$, $k_{i,2} = 3$, $k_{n,3} = 5$, $k_{p,3} = 3$, $k_{i,4} = k_{i,5} = k_{i,6} = 20$, $\lambda_i = 10$, $\gamma_{ij,\theta} = \gamma_{ij,\psi} = 0.1$, $\gamma_{ij,o1} = \gamma_{ij,o2} = 1$, $\gamma_{nj,a} = 0.1$, and $\gamma_{pj,a} = 0.01$ where $i = 1, 2, 3$, $n = 1, 2$, and $p = 3$. The performance functions are selected as $\rho^U_{10,1} = (2.2 - 0.1)e^{-0.2t} + 0.1$, $\rho^L_{10,1} = (1 - 0.1)e^{-0.2t} + 0.1$, $\rho_{10,2} = (\pi - 0.5)e^{-0.1t} + 0.5$, $\rho_{10,3} = \rho_{20,3} = (2\pi - 0.1)e^{-0.3t} + 0.1$, $\rho_{10,4} = \rho_{20,4} = (10 - 0.1)e^{-0.3t} + 0.1$, $\rho_{10,5} = \rho_{32,5} = (100 - 0.5)e^{-0.01t} + 0.5$, $\rho_{10,6} = \rho_{20,6} = (10 - 0.1)e^{-0.3t} + 0.1$, $\rho^U_{20,1} = (4 - 0.1)e^{-0.3t} + 0.1$, $\rho^L_{20,1} = (2 - 0.1)e^{-0.3t} + 0.1$, $\rho_{20,2} = (\pi - 0.5)e^{-0.01t} + 0.1$, $\rho_{20,5} = (50 - 0.5)e^{-0.01t} + 0.5$, $\rho^U_{32,1} = (4.5 - 0.1)e^{-0.03t} + 0.1$, $\rho^L_{32,1} = (2 - 0.1)e^{-0.03t} + 0.1$, $\rho_{32,2} = (\pi - 0.5)e^{-0.01t} + 0.5$, $\rho_{32,3} = (2\pi - 0.1)e^{-0.03t} + 0.1$, $\rho_{32,4} = (20 - 0.1)e^{-0.03t} + 0.1$, and $\rho_{32,6} = (20 - 0.1)e^{-0.03t} + 0.1$. The desired distances and angles are set to $l_{10,r} = 4$, $l_{20,r} = l_{32,r} = 5$, $\theta_{10,r} = \pi/4$, and $\theta_{20,r} = \theta_{32,r} = -\pi/4$. The initial positions of the USVs are chosen as $q_o = [0, 0, 0]^\top$, $q_1 = [0, -5, 0]^\top$, $q_2 = [0, 5, 0]^\top$, and $q_3 = [-5, 5, 0]^\top$ and the path of the global leader q_0 is generated by $\varpi_0 = [0.2, 0, 0]^\top$ for $0 \leq t < 20$, $\varpi_0 = [0.2, 0, -0.1\sin(\pi t/20)]^\top$ for $20 \leq t < 60$, and $\varpi_0 = [0.2, 0, 0]^\top$ for $60 \leq t < 200$.

To show the effectiveness of the proposed leader–follower formation tracking scheme, we simulate with two cases:

Case 1: In this case, it is assumed that there is no proposed obstacle and collision avoidance algorithm. For the simulation under this assumption, $\theta_{ij,d}$ in (7) is set to $\theta_{ij,r}$ and $\rho^L_{32,1}(t_0)$ is changed to 4.4 from 2 so that the condition (21) for collision avoidance is violated. The minimum avoidance ranges are set to $R_{1,m} = R_{2,m} = 1.5$ and $R_{3,m} = 3$. The simulation results are shown in Fig. 3. In Fig. 3(b) and (c), we can observe that there exist time intervals with $l_{1,b} < R_{1,m} = 1.5$ and $l_{32} < R_{3,m} = 3$. These results indicate that there is a risk of collision if there is no proposed collision avoidance algorithm. Fig. 3(a), (c), and (d) show that the proposed algorithm can achieve the desired formation and the connectivity maintenance among USVs, except the collision instant between USV 2 and USV 3.

Case 2: In this case, we verify the performance of the proposed leader–follower formation tracking scheme for collision and obstacle avoidances. To this end, we use the settings mentioned at the beginning of this section and $\gamma_{i,b}$ is to set 0.1. Fig. 4 shows the simulation results. Compared with Fig. 3, it can be seen that the obstacle and collision avoidance is successfully achieved in Fig. 4(a)–(c). Fig. 4(b) and (c) show that the obstacle avoidance condition $l_{1,b} > R_{1,m} = 1.5$ and the collision avoidance condition $l_{32} > R_{3,m} = 3$ are ensured. In addition, Fig. 4(c) and (d) reveal that the connectivity among USVs is maintained during the collision avoidance. Fig. 5 shows that the formation errors remain within the connectivity-maintaining and collision-avoiding performance functions and converge to nearby zero. The control inputs are shown in Fig. 6. In Fig. 4(a), the USV q_3 follows the USV q_2 by the communication connectivity shown in Fig. 2. The curved path of the leader signal is changed to the straight path at 60 s. Then, the velocity of q_2 is adjusted to follow the path change of the leader signal. Thus, the velocity of q_3 is successively adjusted to follow the path change of q_2. In this procedure, the oscillation occurs to reduce the formation error between q_2 and q_3 in the surge force $\tau_{3,u}$. We can conclude that all the results mentioned in Theorem 1 are demonstrated from the simulation results.

5. Conclusions

A connectivity-maintaining and collision-avoiding performance function approach for the robust leader–follower formation tracking has been presented for ensuring connectivity preservation and collision avoidance in achieving the desired formation of multiple uncertain USVs. The novel formation error for ensuring connectivity preservation, collision avoidance, and predesignated formation tracking performance has been derived to design the robust underactuated control laws using only relative state information for each USV where adaptive and approximation techniques are not employed. Moreover, a novel obstacle avoidance strategy without using the potential functions has been proposed to preserve connectivity to the leader while avoiding the obstacle. The stability of the resulting formation control system has been analyzed via Lyapunov stability theorem.

References

Ajorlou, A., & Aghdam, A. G. (2013). Connectivity preservation in nonholonomic multi-agent systems: a bounded distributed control strategy. *IEEE Transactions on Automatic Control*, *58*(9), 2366–2371.

Ajorlou, A., Momeni, A., & Aghdam, A. G. (2010). A class of bounded distributed control strategies for connectivity preservation in multi-agent systems. *IEEE Transactions on Automatic Control*, *55*(12), 2828–2833.

Atinç, G. M., Stipanović, D. M., Voulgaris, P. G., & Karkoub, M. (2013). Collision-free trajectory tracking while preserving connectivity in unicycle multi-agent systems. In *Proc. American Cont. Conf.* (pp. 5392–5397).

Bechlioulis, C. P., & Rovithakis, G. A. (2014). A low-complexity global approximation-free control scheme with prescribed performance for unknown pure feedback systems. *Automatica*, *50*, 1217–1226.

Chaw, D. (2011). Global tracking control of underactuated ships with input and velocity constraints using dynamic surface control method. *IEEE Transactions on Control Systems Technology*, *19*(6), 1357–1370.

Chen, L., Cui, R., Yang, C., & Yan, W. (2019). Adaptive neural network control of underactuated surface vessels with guaranteed transient performance: Theory and experimental results. *IEEE Transactions on Industrial Electronics*, http://dx.doi.org/10.1109/TIE.2019.2914631.

Cortés, J., Martínez, S., & Bullo, F. (2006). Robust rendezvous for mobile autonomous agents via proximity graphs in arbitrary dimensions. *IEEE Transactions on Automatic Control*, *51*(8), 1289–1298.

Cui, R., Ge, S. S., How, B. V. E., & Choo, Y. S. (2010). Leader-follower formation control of underactuated autonomous underwater vehicles. *Ocean Engineering*, *37*(17–18), 1491–1502.

Dai, S., He, S., Wang, M., & Yuan, C. (2019). Adaptive neural control of underactuated surface vessels with prescribed performance guarantees. *IEEE Transactions on Neural Networks and Learning Systems*, http://dx.doi.org/10.1109/TNNLS.2018.2876685.

Do, K. D. (2011). Practical formation control of multiple underactuated ships with limited sensing ranges. *Robotics and Autonomous Systems*, *59*(6), 457–471.

Do, K. D., & Pan, J. (2005). Global tracking of underactuated ships with nonzero off-diagonal terms. *Automatica*, *41*, 87–95.

Dong, J.-G. (2016). Finite-time connectivity preservation rendezvous with disturbance rejection. *Automatica*, *71*, 57–61.

Fiedler, M. (1973). Algebraic connectivity of graphs. *Czechoslovak Mathematical Journal*, *23*(2), 298–305.

Ganguli, A., Cortés, J., & Bullo, F. (2009). Multirobot rendezvous with visibility sensors in nonconvex environments. *IEEE Transactions on Robotics*, *25*(2), 340–352.

Gennaro, M. C. D., & Jadbabaie, A. (2016). Decentralized control of connectivity for multi-agent systems. In *Proc. 45th IEEE Int. Conf. decision control* (pp. 3628–3633).

Ghommam, J., & Saad, M. (2018). Adaptive leader-follower formation control of underactuated surface vessels under asymmetric range and bearing constraints. *IEEE Transactions on Vehicular Technology*, *67*(2), 852–865.

Giordano, P. R., Franchi, A., Secchi, C., & Bülthoff, H. H. (2013). A passivity-based decentralized strategy for generalized connectivity maintenance. *International Journal of Robotics Research*, *32*(3), 299–323.

Huang, C., Zhang, X., & Zhang, G. (2019). Improved decentralized finite-time formation control of underactuated USVs via a novel disturbance observer. *Ocean Engineering*, *174*(15), 117–124.

Jin, J., Kim, Y., Wee, S., & Gans, N. (2015). Decentralized cooperative mean approach to collision avoidance for nonholonomic mobile robots. In *Proc. IEEE Int. Conf. robotics and automation* (pp. 35–41).

Karkoub, M., Atinć, G., Stipanovic, D., Voulgaris, P., & Hwang, A. (2019). Trajectory tracking control of unicycle robots with collision avoidance and connectivity maintenance. *Journal of Intelligent and Robotic Systems*, *96*, 331–343.

Li, X., Sum, D., & Yang, J. (2013). A bounded controller for multirobot navigation while maintaining network connectivity in the presence of obstacles. *Automatica*, *49*(1), 285–292.

Moe, S., & Pettersen, K. Y. (2016). Set-based line-of-sight (LOS) path following with collision avoidance for underactuated unmanned surface vessel. In *Proc. 24th Mediterranean Conf. control and automation*. Athenes, Greece, (pp. 402–409).

Park, B. S. (2015). Adaptive formation control of underactuated autonomous underwater vehicles. *Ocean Engineering*, *96*, 1–7.

Park, B. S., Kwon, J., & Kim, H. (2017). Neural network-based output feedback control for reference tracking of underactuated surface vessels. *Automatica*, *77*, 353–359.

Park, B. S., & Yoo, S. J. (2019). An error transformation approach for connectivity-preserving and collision-avoiding formation tracking of networked uncertain underactuated surface vessel. *IEEE Transactions on Cybernetics*, *49*(8), 2955–2966.

Peng, Z., Wang, D., Chen, Z., Hu, X., & Lan, W. (2013). Adaptive dynamic surface control for formations of autonomous surface vehicles with uncertain dynamics. *IEEE Transactions on Control Systems Technology*, *21*(2), 513–520.

Poonawala, H. A., Satici, A. C., Eckert, H., & Spong, M. W. (2015). Collision-free formation control with decentralized connectivity presrevation for nonholonomic-wheeled mobile robots. *IEEE Transactions on Control of Networked Systems*, *2*(2), 122–130.

Qin, H., Li, C., Sun, Y., Li, X., Du, Y., & Deng, Z. (2019). Finite-time trajectory tracking control of unmanned surface vessel with error constraints and input saturations. *Journal of the Franklin Institute*, http://dx.doi.org/10.1016/j.jfranklin.2019.07.019.

Sabattini, L., Secchi, C., Chopra, N., & Gasparri, A. (2013). Distributed control of multirobot systems with global connectivity maintenance. *IEEE Transactions on Robotics*, *29*(5), 1326–1332.

Sakai, D., Fukushima, H., & Matsuno, F. (2018). Leader-follower navigation in obstacle environments while preserving connectivity without data transmission. *IEEE Transactions on Control Systems Technology*, *26*(4), 1233–1248.

Shojaei, K. (2015). Leader–follower formation control of underactuated autonomous marine surface vehicles with limited torque. *Ocean Engineering*, *105*, 196–205.

Skjetne, R., Fossen, T. I., & Kokotović, P. V. (2005). Adaptive maneuvering, with experiments, for a model ship in a marine control laboratory. *Automatica*, *41*(2), 289–298.

Su, H., Wang, X., & Chen, G. (2010). Rendezvous of multiple mobile agents with preserved network connectivity. *Systems & Control Letters*, *59*(5), 313–322.

Sun, Z., Zhang, G., Lu, Y., & Zhang, W. (2018). Leader-follower formation control of underactuated surface vehicles based on sliding mode control and parameter estimation. *ISA Transactions*, *72*, 15–24.

Sun, Z., Zhang, G., Yang, J., & Zhang, W. (2018). Research on the sliding mode control for underactuated surface vessels via parameter estimation. *Nonlinear Dynamics*, *91*(2), 1163–1175.

Xie, W., & Ma, B. (2018). A new formation control of multiple underactuated surface vessels. *International Journal of Control*, *91*(5), 1011–1022.

Xie, W., Ma, B., Huang, W., & Zhao, Y. (2018). Global trajectory tracking control of underactuated surface vessels with non-diagonal inertial and damping matrices. *Nonlinear Dynamics*, *92*(4), 1481–1492.

Yoo, S. J., & Park, B. S. (2017). Guaranteed performance design for distributed bounded containment control of networked uncertain underactuated surface vessels. *Journal of the Franklin Institute*, *354*(3), 1584–1602.

Zavlanos, M. M., Tanner, H. G., Jadbabaie, A., & Pappas, G. J. (2009). Hybrid control for connectivity preserving flocking. *IEEE Transactions on Automatic Control*, *54*(12), 2869–2875.

Bong Seok Park received his B.S., M.S., and Ph.D. degrees in Electrical and Electronic Engineering from Yonsei University in 2005, 2008, and 2011, respectively. Since 2015, he has been with the Division of Electrical, Electronic, and Control Engineering, Kongju National University. His research interests include nonlinear control, formation control, and the control of robots.

Sung Jin Yoo received his B.S., M.S., and Ph.D. degrees in Electrical and Electronic Engineering from Yonsei University, Seoul, South Korea, in 2003, 2005, and 2009 respectively. He has been a Post-doctoral researcher in the Department of Mechanical Science and Engineering, University of Illinois at Urbana–Champaign, Illinois from 2009 to 2010. Since 2011, he has been with the School of Electrical and Electronics Engineering, ChungAng University, Seoul, South Korea where he is currently a Professor. His research interests include nonlinear adaptive control, decentralized control, distributed control, fault-tolerant control, and neural networks theories, and their applications to robotic, flight, nonlinear time-delay systems, large-scale systems, and multi-agent systems.